3D Microfabrication of Photosensitive Resin Reinforced with Ceramic Nanoparticles Using LCD Microstereolithography

Dongkeon Lee, Takashi Miyoshi, Yasuhiro Takaya and Taeho Ha

Division of Production and Measurement System Engineering, Department of Mechanical Engineering and Systems, Graduate School of Engineering, Osaka University, 2-1 Yamada-oka, Suita-shi, Osaka 565-0871, Japan
E-mail: miyoshi@mech.eng.osaka-u.ac.jp

A new liquid crystal display (LCD) microstereolithography process has been developed in order to fabricate microparts with superior mechanical properties (for e.g., micro gears). In this paper, we investigate the fabrication process of micro bevel gears using photosensitive resins reinforced with ceramic nanoparticles; these are made by uniformly mixing ceramic nanoparticles with photosensitive resins. A reduction in surplus growth is required for the improvement of the form accuracy of the micro bevel gears. The reduction in the surplus growth is accomplished as follows. First, the partially solidified resin is gently removed using the forced flow of the developed resin; this forced flow is controlled by the stage that moves along the Z-axis (Z-stage). Second, the exposure procedure for grayscale LCD masks is performed to reduce the surplus growth caused by a repetitive lamination procedure. Finally, the continuous lamination microstereolithography method using a grayscale LCD mask enables the production of highly precise microstructures such as micro bevel gears within a maximum error rate of 3.6%.

Keywords: ceramic nanoparticles, photosensitive resin, microstereolithography, grayscale, LCD mask

1. Introduction

Recently, microstereolithography (μ-STL) technologies have been rapidly developing in the field of microelectromechanical systems (MEMS) [1–3]. In addition, with regard to the application of photosensitive resins, the use of resins reinforced with ceramic particles has been proposed to fabricate a ceramic 3D structure by μ-STL [4–8]. The μ-STL has advantages similar to the conventional stereolithography techniques, such as the flexibility of the fabrication structure and compatibility with a computer-aided design (CAD) system. The disadvantage of this method, however, is the poor mechanical strength owing to the only use of photosensitive resins [9–11]. Furthermore, it is difficult to improve both the mechanical strength and processing accuracy. In this report, we propose a novel method in order to overcome the abovementioned disadvantages; this involves the continuous lamination μ-STL method using a liquid crystal display (LCD) mask and photosensitive resins reinforced with ceramic nanoparticles. Thus, the purpose of this research is to improve both the mechanical strength and processing accuracy by using our proposed method.

The novelty of this method lies in the application of a grayscale mask pattern displayed on the LCD mask in order to reduce the surplus growth that worsens the processing accuracy. First, a micro bevel gear is fabricated for the evaluation of the processing accuracy and mechanical strength of the microparts. The shapes of the gear being similar to those of typical mechanical elements, these are suitable for the evaluation of the surplus growth since this growth is easily generated on the surface of both the center hole and teeth. In order to verify the effectiveness of this method, we fabricate the micro bevel gear with a high processing accuracy, high mechanical strength, and without the surplus growth.

2. Continuous lamination microstereolithography method using an LCD mask

The schematic diagram of the continuous lamination microstereolithography method using an LCD mask is shown in Fig.1. The micro bevel gears are first designed using a 3D CAD system. Next, a
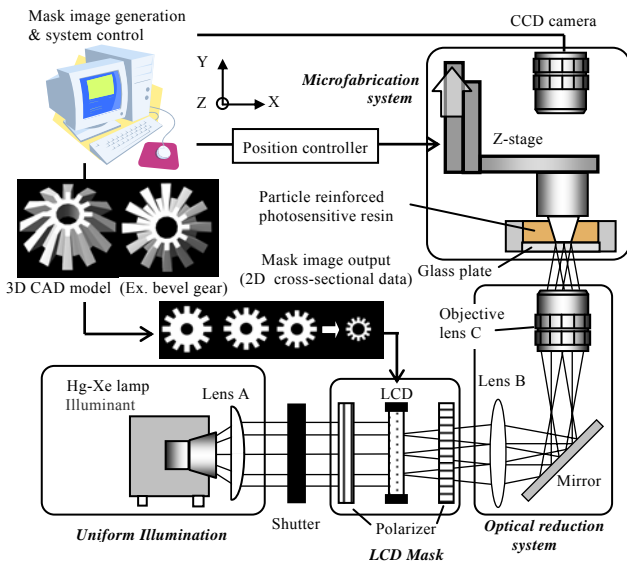
Fig. 1 Schematic diagram of the experimental apparatus.

series of 2D cross-sectional data is generated from the 3D CAD model of a micro bevel gear. These cross-sectional data are used as the dynamical mask pattern for the LCD mask. The experimental apparatus mainly consists of a uniform illumination system, an LCD mask system, an optical reduction system, and a fabrication system with a Z-stage for the lamination procedure.

An Hg-Xe lamp is used as the light source; this source provides the strongest light intensity at a wavelength of 436nm. The photosensitive resin used in this experiment is highly sensitive to this wavelength. The irradiation from the light source is collimated by passing it through the collimating lens A; the collimated beam then uniformly illuminates the LCD mask, which is placed between two quarter-wave plates. Next, the gear pattern displayed on the LCD is reduced to 16% of its size by using the optical reduction system that comprises the condenser lens B and the imaging lens C. The reduced image is then focused onto the glass plate at the bottom of a resin container. Synchronizing the Z-stage movement with the cross-sectional data of a gear makes the successive lamination procedures from the first layer to the final layer possible. The 3D micro bevel gear is finally fabricated by using this system.

3. Evaluation of the µ-STL processability of the photosensitive resin reinforced with ceramic nanoparticles

3.1 Photopolymerization characteristics of the photosensitive resin reinforced with ceramic nanoparticles

The Vickers hardness value (40.1 HV) of the photosensitive resin reinforced with ceramic nanoparticles is as high as 3.4 times that of the

photosensitive resin (KC1042, Japan Synthetic Rubber Co., Ltd.) used for the base material of the developed resin. The chemical composition of the photosensitive resin reinforced with ceramic nanoparticles is as follows.

◈ Particles
  Al_2O_3-SiO_2 (50wt%, average diameter, 98 nm)
◈ Photosensitive resin
  KC1042 (9.4wt%, urethane-acrylic)
  KC1162 (37.6wt%, made of a monomer with a
        highly dense acrylic functional group)
◈ Dispersant
  Hydrophobic polymer (1.5wt%)
  Phosphate ester monomer (1.5wt%)

Basic experiments are conducted to examine the photopolymerization characteristics of the developed resin. Fig.2 shows the relationship between the cure depth and the exposure energy for the photosensitive resin reinforced with ceramic nanoparticles and the dispersant. The cure depth is 28.9 µm at an exposure energy of 5 mJ/cm^2; this is almost equivalent to the minimum exposure energy used in this method. The developed resin thus has a cure depth sufficient to fabricate 3D microparts because the layer thickness is usually less than 10 µm in microstereolithography. The cure depth is calculated from equation (1) according to the Beer-Lambert law.

$$C_d = D_p \ln(E / E_c) \qquad (1)$$

Here, C_d is the cure depth; D_p, the penetration depth of the beam; and E, the exposure energy per unit surface area of the resin. The quantity E_c is the critical exposure energy for the resin. The incident light is widely scattered and absorbed within the photosensitive resin reinforced with ceramic nanoparticles.
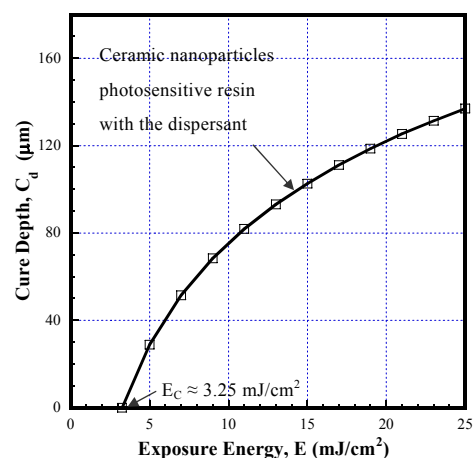

Fig. 2 Relationship between the cure depths and the exposure energies and the influence of dispersants.
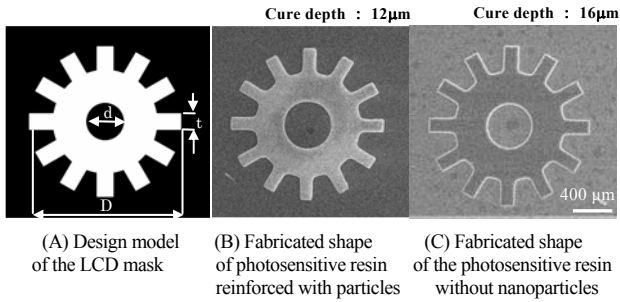
Fig. 3 Cure depths and dimensions according to the extent of mixing of the ceramic nanoparticles.

Table 1 Dimensions of each fabricated part (Unit: μm)

	A	B	C
Tooth width (t)	179	133	156
Diameter (D)	1620	1540	1620
Hole diameter (d)	400	468	440

It is thought that the light scattering and absorption within the resin cause a decreased cure depth. The scattered light also worsens the processing accuracy. The interlayer adhesion thus decreases.

Fig.3 shows a typical result that could be based on the abovementioned phenomenon. Fig.3 (A) shows the pictures of the exposed mask pattern. Figs.3 (B) and (C) show the gear shapes fabricated at an exposure energy of 12.0 mJ/cm^2 by using the photosensitive resins with and without nanoparticles, respectively. A comparison of the fabricated shapes of (B) and (C) shown in Table 1 reveals that the gear with nanoparticles (B) is smaller by 23 μm in the tooth width (t) and by 80 μm in the diameter (D); however, its hole diameter is larger by 28 μm.

Thus, it is considered that the solidification of the gear shape is not completed in the case of the photosensitive resin reinforced with ceramic particles. Therefore, a higher exposure energy is required for the fabrication of the microparts as compared to that of the photosensitive resin without nanoparticles.

3.2 The continuous lamination characteristics of micro bevel gears according to the change in exposure energy

A 50-layer lamination with successive exposures is performed by varying the exposure energy in order to examine the processing accuracy of the micro bevel gear. The illumination intensity is 103.5 mW/cm^2. The exposure time for each layer is varied at 0.04 s (T$_A$), 0.09 s (T$_B$), 0.13 s (T$_C$), and 0.18 s (T$_D$).

Fig.4 shows the results of the exposure of the mask pattern of the gear to varying exposure times and also shows the fabrication results of the micro bevel gear consisting of 50 layers. Table 2 shows the influence of the exposure energy on the dimensional errors (%) for a single exposure and for 50 exposures.
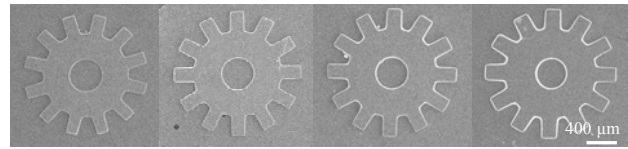
(A) 0.04 s/layer   (B) 0.09 s/layer   (C) 0.13 s/layer   (D) 0.18 s/layer

[1st layer fabrication] Layer thickness, 10 μm; number of layers, 1
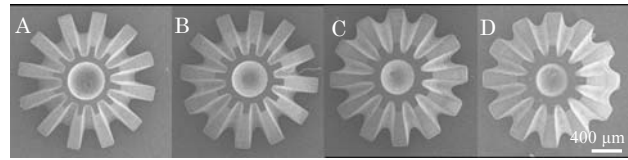
[Laminating fabrication] Layer thickness, 10 μm; numbers of layers, 50

Fig. 4 Micro bevel gears fabricated with a single (1st) layer and by lamination.

Table 2 Evaluation of the processing accuracy and laminating ability

No.	Exposure energy (mJ/cm^2)	Error rates of cured parts (%)						Processing accuracy		Surplus growth	
		Diameter (D)		Tooth width (t)		Hole diameter (d)					
		1st	50th	1st	50th	1st	50th	1st	50th	tooth	hole
A	4.6	-1.9	-0.2	-13.4	-22.0	-8.5	-8.0	×	×	○	×
B	9.1	-0.6	+0.6	-1.1	-7.7	-0.8	-5.1	○	△	△	×
C	13.8	+0.6	+0.8	+1.1	+1.1	-0.5	-0.2	○	○	×	×
D	18.3	+1.2	+2.0	+10.6	+4.4	+7.3	+4.6	×	×	×	×

○: Excellent, △: Good, ×: Poor

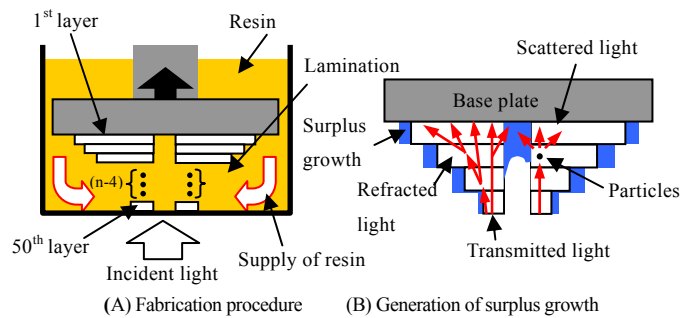(A) Fabrication procedure   (B) Generation of surplus growth

Fig. 5 Generation mechanism of surplus growth in the microfabrication.

From the above results, the dimensional error (%) is observed to be less than 1.1% in the case of C (shown in Table 2) as compared to the designed shape displayed on the LCD mask. However, a large surplus growth is observed on the tooth surface in the case of C as compared to that of B.

Fig.5 schematically shows the generation mechanism of the surplus growth in the fabrication of the micro bevel gear. This gear has the largest exposure area on the first layer. The exposure area gradually decreases with a reduction rate of 1% up to the last (50th) layer.
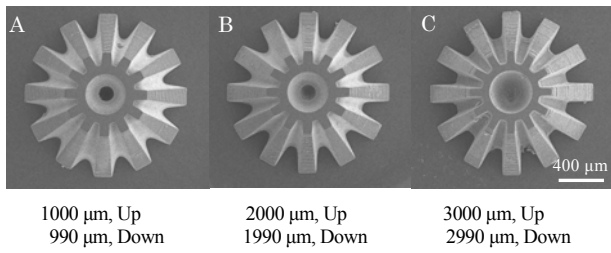
1000 μm, Up 2000 μm, Up 3000 μm, Up
990 μm, Down 1990 μm, Down 2990 μm, Down

Fig.6 Fabrication results according to the distance through which the Z-stage is moved.

Fig. 7 The relationship between exposure intensities and grayscales.

While processing the lamination of the layers under successive exposures, the incident light is scattered by the nanoparticles and the boundary between layers. The scattered light is transmitted through previously hardened layers among those formed towards the end of the process. It could be thought that the surplus growth is generated at the bottom of the center hole or between the teeth because of the reflection of light on the base plate and the light scattered by the solidified layers.

3.3 Investigation of the Z-stage movement on the fabrication characteristics

The partially solidified resin on the gear surface requires to be removed in order to reduce the surplus growth. This is accomplished by supplying fresh photosensitive resin between the gear surface and exposure plane. In spite of the high viscosity of the photosensitive resin reinforced with ceramic nanoparticles, this can be done as follows. First, the base plate in the resin container controlled by the Z-stage is moved higher upward and then allowed to descend to the desired layer thickness.

The experimental results of successive laminating fabrication of the micro bevel gears with varying distance of the Z-stage are shown in Fig.6. An exposure energy of 13.7 mJ/cm^2 is used, which corresponds to the best processing accuracy of case (C) in Table 1. The thickness of each layer and the total number of continuous laminations are 10 μm and 50.

The upward distances of the experimental conditions A, B, and C are 1000 μm, 2000 μm, and 3000 μm, respectively, and the descending distances are 990 μm, 1990 μm, and 2990 μm, respectively. The smooth supply of the resin with a high viscosity becomes easier by increasing the distance through which the Z-stage is moved. It is possible to generate a thin uniform resin layer with a thickness of 10 μm in this method. On the other hand, in spite of the reduction in the surplus growth on the tooth surface, the generation of the surplus growth in the center hole is not sufficiently retarded, as shown in Fig.6.

Presently, the maximum velocity of the Z-stage in this experiment is 4 mm/s, and the total fabrication time
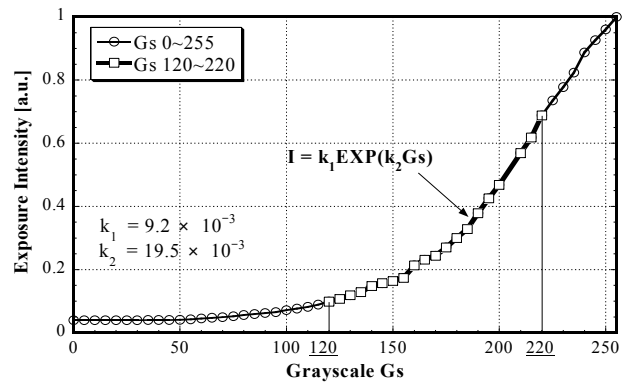
of the experimental conditions A, B, and C is 11 min, 17 min, and 25 min, respectively.

4. The effect of grayscale

4.1 Relationship between grayscale and the exposure intensity

We propose an LCD mask microstereolithography method using the grayscale mask pattern. The grayscale LCD mask is capable of controlling the distribution of the exposure energy to reduce the surplus growth both in the center hole and on the tooth surface.

The exposure intensity is examined by varying the grayscale level. Fig.7 shows the relationship between the exposure intensity and the grayscale level. The exposure intensity is normalized by the intensity at a grayscale level of 255. The intensity is kept almost constant up to a grayscale level of 100. The exposure intensity then exponentially increases with an increase in the grayscale level in the range of 120 to 220. This relationship agrees well with the approximating curve based on equation (2) as expressed below.

$$I = k_1 \exp(k_2 Gs) \qquad (2)$$

Here, k_1 and k_2 are constants; $k_1 = 9.2 \times 10^{-3}$, $k_2 = 19.5 \times 10^{-3}$.

4.2 Cure characteristics according to the shape of the grayscale mask and the ratio of gray values

We investigate the effect of the grayscale mask patterns on the reduction of the surplus growth. Fig.8 shows the gear shapes fabricated by the two different shapes of the grayscale mask patterns: the grayscale pattern is 85% reduced gear shape (A) and the other is shaped like a circle (B) surrounding the center hole. The grayscale level is of the same value (160) in both the shapes. The fabrication conditions are as follows. The exposure energy is 13.8 mJ/cm^2; the layer thickness, 10 μm; and the lamination number, 5.
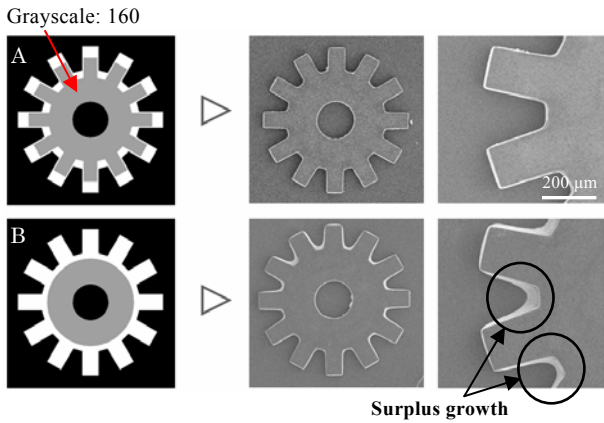
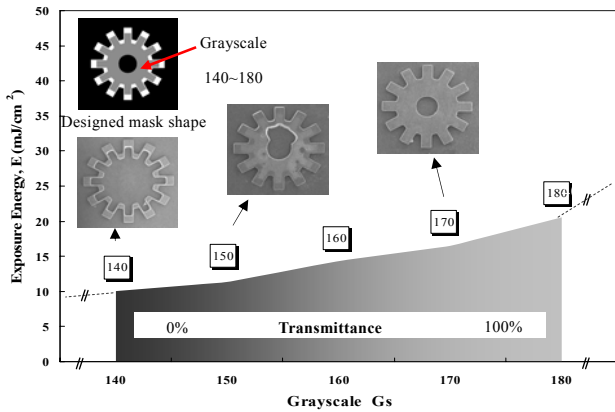**Fig. 8** Fabrication results according to the grayscale mask.

Fig. 9 Fabrication characteristics according to grayscales.

Fig. 10 Laminating fabrication results according to grayscales.

Table 3 Evaluation of laminating fabrication results

Gray scale	Layer	Error rates of cured parts (%)			Processing accuracy	Surplus growth	
		Diameter (D)	Tooth width (t)	Hole diameter (d)		Tooth	Hole
160	1st	-0.6	-2.2	-8.4	△	△	×
	50th	-0.6	-2.5	-3.7	△		
170	1st	-0.5	-1.1	-0.3	○	○	×
	50th	-0.2	-1.1	-1.7	○		

○: Excellent, △: Good, ×: Poor
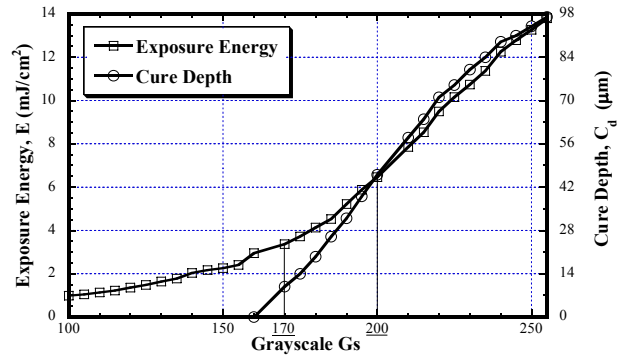
Fig. 11 Relationships among cure depths, grayscales, and exposure energies.

With regard to the fabrication of the tooth part, the gear shape created using the grayscale mask A has a good processability without the generation of the surplus growth as compared to that created using the grayscale mask B. As a result, applying the grayscale mask pattern (A) is effective in reducing the surplus growth.

Fig.9 shows the fabrication results obtained by increasing the grayscale level from 140 to 180 by using the grayscale mask shown in Fig.8 (A). The longitudinal axis indicates the sum of the total exposure energies during the five exposures, and the lateral axis indicates the grayscale and the light transmission (%) corresponding to the grayscale. In the case of the grayscale levels of 140 and 150, the fabrication is not successful; this is because the exposure energy is less than the critical exposure energy as a consequence of the law of transmittance for the LCD mask.

Fig.10 shows the results of the continuous lamination performed 50 times; the results are depicted using the grayscale mask (as shown in Fig.8 (A)) with grayscale levels of 140, 160, 170, and 180, respectively. The portion around the center hole is not solidified at the grayscale level of 140. On the other hand, a large surplus growth is generated in the center hole at the grayscale level of 180.
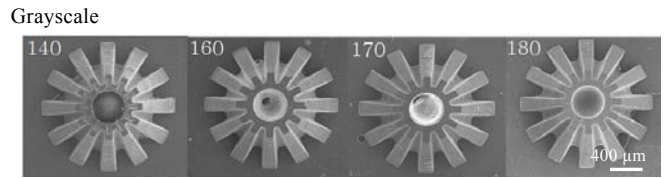
The fabrication results for the grayscale levels of 160 and 170 show a good processability, as shown in Table 3. The maximum error rate is less than 2%, and the best processing accuracy is obtained in the case of the grayscale level of 170. The micro bevel gear is finally fabricated without the surplus growth on the tooth surface. The surplus growth, however, still remains in the center hole since the incident light scatters from the particles in the cured layer and penetrates the boundary of the interlayer.

4.3 Fabrication results

In this section, we develop the grayscale mask patterns that enable the reduction of the surplus growth in the center hole. Fig.11 illustrates the relationship between the grayscale levels and the exposure energies or the cure depths, which is obtained from the results shown in Figs.2 and 7. The cure depth linearly increases up to a grayscale level of 220. The grayscale level of 255 (maximum value) is equivalent to the exposure energy of 13.8 mJ/cm^2 and is the value that is able to fabricate the first layer with a high processing
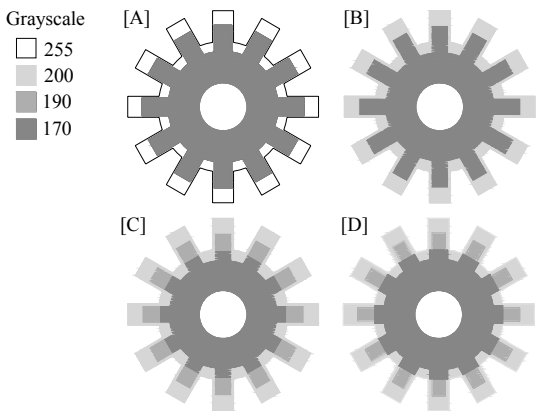
Fig. 12 LCD mask images designed for various grayscales.

Fig. 13 The fabricated micro bevel gear having a layer thickness of 10 μm.

Table 4 Dimensions of the fabricated micro bevel gear

Layer	Error rates of cured parts (%)			Processing accuracy
	Diameter (D)	Tooth width (t)	Hole diameter (d)	
1st	-0.5	-1.1	-0.3	○
50th	-1.6	-3.6	-0.6	△

accuracy. The critical exposure energy (Ec), which is the threshold value to cure the resin, is approximately 3 mJ/cm² and corresponds to the grayscale level of 160 in Fig.11. An exposure energy of over 3.53 mJ/cm² at a grayscale level of 170 is required for a cure depth of 10 μm. The thickness of the curable resin reaches up to 45 μm when the exposure energy is 6.5 mJ/cm² at a grayscale level of 200; in this case, stable laminating fabrications become possible.

It would appear that the masks with a grayscale range from 170 to 200 are suitable for decreasing the surplus growth in the center hole because of the reduction in the extra energy to generate the surplus growth. A grayscale level of over 200 is recommended for the fabrication of the tooth edge because the discontinuous concavo-convex zone with a narrow exposure area like those of the tooth parts is required to have a higher intensity than that at the inner side.

According to the abovementioned discussions, several mask patterns are finally designed for the fabrication of the micro bevel gear; these include a higher grayscale level in the tooth part and a lower one in the center hole. The maximum and minimum values of the grayscale levels are 255 and 170, respectively. Multigrayscale masks are required for the microfabrication of micro bevel gear without the surplus growth in the center hole or on the tooth surface.

Four types of grayscale masks are prepared, as shown in Fig.12. The grayscale levels are divided into four—255, 200, 190, and 170. The mask of pattern A has a grayscale level of 255 in the tooth portion and 170 in the inner portion. Pattern B has a level of 200 in the tooth portion and 170 in the inner portion. Patterns C and D have level of 200 in the tooth portion, 190 in the middle of this portion, and 170 in the inner side. The area of the tooth portion with a grayscale level of 190 is different in patterns C and D. At the tooth edge, pattern D has a higher transmittance than pattern C.
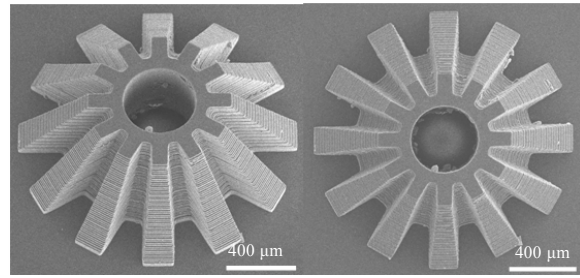
Pattern A has a good processability in the tooth region and center hole and is used for the fabrication of the 1st to 19th layers. Patterns B, C, and D with different grayscale values are used for the 20th to 50th layers because the surplus growth increases after the exposure of the 20th layer. The distance moved by the Z-stage is 5 mm; the layer thickness, 10 μm; and the fabrication time, 38 min. From the fabrication results obtained by using the masks of B, C, and D, micro bevel gears can be produced without surplus growth on the tooth surface and center hole. This means that the grayscale level in the inner region of the center hole should be set at a lower value than that in the outer region. In order to control the surplus growth in the center hole the appropriate grayscale level is 200 in the outer portion and 170 inside. It is recognized that the appropriate grayscale level also represses the refracted and scattered light intensity in the inner layers despite the number of exposures being over 30. In the tooth region, the processing accuracies of B, C, and D have error rates of 9.1%, 4.3%, and 3.6%, respectively. It is found that pattern D gives the highest accuracy and that a grayscale with three gradients is better than that with two gradients. The grayscale should be set to gradually decrease from the outside. Furthermore, it is suggested that the processing accuracy is also affected by the grayscale mask area.

Fig.13 shows scanning electron microscopy (SEM) images of the micro bevel gear fabricated by grayscale mask D, which has the best accuracy in the error rates for the 1st and 50th layer laminations. The micro bevel gear with a clear center hole and tooth region can be observed without the surplus growth.

Table 4 shows the error rates in the three typical features of the gear. The dimensions of the micro bevel gear are within the error rate of –0.3% in the center hole of the first layer. The surplus growth is reduced to a small error rate of –0.6% in the case of the 50th layer. The micro bevel gear is fabricated with a small dimension error of less than 3 μm in the center hole having a diameter of 400 μm.

5. Conclusions

The conclusions are summarized as follows.

1) The continuous lamination system based on LCD grayscale mask microstereolithography is established for the fabrication of 3D microparts using photosensitive resin reinforced with ceramic nanoparticles.

2) This resin is developed by mixing ceramic nanoparticles with an average particle diameter of 90 nm with photosensitive resin. Based on the micro-Vickers hardness test, the hardness of the solidified resin including the nanoparticles is found to be as high as 3.4 times that of the resin without the particles.

3) The resin that was developed satisfied the criteria of both good dispersibility and high fluidity. A repetitive lamination procedure for the formation of 50 layers is successively performed to obtain a layer thickness of 10 μm.

4) The exposure time for each layer is less than 0.15 s, and the micro bevel gear consisting of 50 layers can be quickly fabricated within error rates of 3.6% and with a high processing accuracy.

5) The micro bevel gear with a center hole having a diameter of 400 μm was accurately fabricated within error rates of 2% because of the reduction of the surplus growth generated in the center hole. The surplus growth could be reduced by controlling the grayscale of the LCD mask.

Based on the above results, we confirmed the effectiveness of the LCD grayscale mask microstereolithography method using photosensitive resins reinforced with ceramic nanoparticles.

References

[1] Special Issue: The Latest Trends of Rapid Prototyping, J. JSPE, 70, 2, (2004) 163.

[2] V. K. Varadan et al.: "Microstereolithography and Other Fabrication Techniques for 3D MEMS," (John Wiley & Sons, West Sussex, 2001).

[3] T. Kohlmeier, V. Seidemann, S. Bűttgenbach and H. H. Gatzen: Microsystem Technologies, 8, (2002) 304

[4] C. Sun, and X. Zhang: Sens. Actuators A, 101, (2002) 364.

[5] T. Chartier, C. Chartier, F. Doreau, and M. Loiseau: J. of Mater. Sci., 37, (2002) 3141.

[6] S. Monneret, C. Provin, H. Le Gall, and S. Corbel: Microsystem Technologies, 8, (2002) 368.

[7] M. L. Griffith, and J. W. Halloran: J. Am. Ceram. Soc., 78, 10, (1996) 2601.

[8] C. Provin, S. Monnernet, H.L. Gall and S. Corbel: Adv. Mater., 15, 12, (2003), 994.

[9] M. Farsari, F. Claret-Tournier, S. Huang, C.R. Chatwin, D.M. Budgett, P.M. Birch, R.C.D. Young and J.D. Richatdson: J. Mater. Proc. Tech., 107, (2002) 167.

[10] S. Zissi, A. Bertsch, J.Y. Jézéquel, S. Corbel, D.J. Lougnot and J.C. André: Microsystem Technologies, 2, (1996), 97

[11] M. Straub, L.H. Nguyen, A. Fazlic and M. Gu: Optical Materials, 27, (2004), 359